JOURNAL OF NEUROPHYSIOLOGY
Vol. 71, No. 1, January 1994. *Printed in U.S.A.*

Simulator for Neural Networks and Action Potentials: Description and Application

ISRAEL ZIV, DOUGLAS A. BAXTER, AND JOHN H. BYRNE
Department of Neurobiology and Anatomy, University of Texas Medical School at Houston, Houston, Texas 77030

SUMMARY AND CONCLUSIONS

1. We describe a simulator for neural networks and action potentials (SNNAP) that can simulate up to 30 neurons, each with up to 30 voltage-dependent conductances, 30 electrical synapses, and 30 multicomponent chemical synapses. Voltage-dependent conductances are described by Hodgkin-Huxley type equations, and the contributions of time-dependent synaptic conductances are described by second-order differential equations. The program also incorporates equations for simulating different types of neural modulation and synaptic plasticity.

2. Parameters, initial conditions, and output options for SNNAP are passed to the program through a number of modular ASCII files. These modules can be modified by commonly available text editors that use a conventional (i.e., character based) interface or by an editor incorporated into SNNAP that uses a graphical interface. The modular design facilitates the incorporation of existing modules into new simulations. Thus libraries can be developed of files describing distinctive cell types and files describing distinctive neural networks.

3. Several different types of neurons with distinct biophysical properties and firing properties were simulated by incorporating different combinations of voltage-dependent Na^+, Ca^{2+}, and K^+ channels as well as Ca^{2+}-activated and Ca^{2+}-inactivated channels. Simulated cells included those that respond to depolarization with tonic firing, adaptive firing, or plateau potentials as well as endogenous pacemaker and bursting cells.

4. Several types of simple neural networks were simulated that included feed-forward excitatory and inhibitory chemical synaptic connections, a network of electrically coupled cells, and a network with feedback chemical synaptic connections that simulated rhythmic neural activity. In addition, with the use of the equations describing electrical coupling, current flow in a branched neuron with 18 compartments was simulated.

5. Enhancement of excitability and enhancement of transmitter release, produced by modulatory transmitters, were simulated by second-messenger–induced modulation of K^+ currents. A depletion model for synaptic depression was also simulated.

6. We also attempted to simulate the features of a more complicated central pattern generator, inspired by the properties of neurons in the buccal ganglia of *Aplysia*. Dynamic changes in the activity of this central pattern generator were produced by a second-messenger–induced modulation of a slow inward current in one of the neurons.

INTRODUCTION

The ability of a neural network to process information and to generate a specific pattern of electrical activity is dependent on both the intrinsic biophysical properties of the individual neurons in the network and their pattern of synaptic connectivity. The specific role that any one process plays in the overall behavior of the network can be difficult to assess due to such factors as interacting nonlinear feedback loops and inaccessibility of the process for experimental manipulation. One way to overcome this problem is to mathematically model and simulate the biophysical and biochemical properties of individual neurons and dynamic properties of the individual synapses. The output of the resynthesized network and its sensitivity to manipulation of individual or multiple variables and parameters can then be examined. To do so, it is necessary to have a flexible simulator that is capable of simulating the important aspects of intrinsic membrane properties, synapses, and modulatory processes. Several simulators are available for simulating realistic neural networks (for review see De Schutter 1992). Some, like SABER (Carnevale et al. 1990) or SPICE (Bunow et al. 1985), were originally designed as general purpose simulators or as simulators of electrical circuits. Simulators such as NEURON (Hines 1989) were designed to simulate dendritic trees of single neurons, whereas others such as GENESIS (Wilson and Bower 1989), NODUS (De Schutter 1989), MacNerveNet (Boney et al. 1991), and NeuronC (Smith 1992) were designed to simulate connections among neurons. Other simulators such as MARIO (Getting 1989) and SLONN (Wang and Hsu 1990) are mainly optimized to simulate integrate-and-fire type neurons. This paper describes a simulator for neural networks and action potentials (SNNAP) that provides a way to simulate the membrane potential of neurons with multiple types of membrane currents. Cells can be interconnected through chemical and/or electrical synapses. Modulatory effects of intracellular ions or extrinsic transmitters can be simulated with equations describing the concentration of different ions and second messengers, the solutions of which drive equations describing the modulation of voltage-dependent conductances. Aspects of synaptic plasticity such as synaptic depression and synaptic facilitation can be simulated as well. Portions of this work have appeared in preliminary form (Ziv et al. 1991, 1992).

METHODS

SNNAP can simulate a network of up to n neurons. Each neuron may include up to m voltage-dependent conductances and up to n electrical and $n \times o$ chemical synapses. Any given presynaptic cell can make up to o chemical synapses with each of its postsynaptic cells. This allows for the simulation of multicomponent synaptic actions. The parameters m, n, and o are limited by the amount of computer memory. m and n were set to 30 and o to 4 in the current version of the program. Voltage-dependent conductances are described by Hodgkin-Huxley type equations, and the contribution of time-dependent synaptic conductances are de-

scribed by second-order ordinary differential equations (ODE). Voltage-dependent conductances can be modulated by linking them to descriptions of the intracellular concentrations of various ions and/or second messengers. Pools of ions and second messengers are simulated as first-order systems. The electrical activity of a simulated neuron or network can be spontaneous or it can be influenced by the injection of depolarizing or hyperpolarizing current or can be modulated by the application of different modulator agents.

Components of the model

MEMBRANE POTENTIAL. The relation between the membrane potential and the membrane current is described by

$$\frac{dV_i}{dt} = -\frac{\sum_{j=1}^{m} Ivd_{ij} + \sum_{k=1}^{n} Ies_{ik} + \sum_{k=1}^{n}\sum_{l=1}^{o} Ics_{iko}}{C_{M_i}} \quad (1)$$

where C_M is the membrane capacitance, V the membrane potential, and *Ivd, Ies,* and *Ics* represent currents due to voltage-dependent conductances, electrical synapses, and chemical synapses, respectively. The parameters n and m represent the total number of neurons and voltage-dependent conductances, respectively, and i, j, k, and l represent the indexes of the neuron, the voltage-dependent conductance, the presynaptic neuron, and the synapse, respectively. An electrical circuit equivalent of this membrane model is illustrated in Fig. 1.

Voltage-dependent conductances. Currents due to voltage-dependent membrane conductances are calculated with the use of

$$Ivd_{ij} = \bar{g}vd_{ij} \cdot A^{p_{ij}} \cdot B_{ij} \cdot \prod_{q=1}^{nr} f[REG_q] \cdot (V_i - Evd_{ij}) \quad (2)$$

where *Evd* is the equilibrium potential, $\bar{g}vd$ is the maximal conductance, A and B are the dimensionless voltage- and time-dependent activation and inactivation terms, and p is the exponent of the activation function. Each *Ivd* can be regulated by nr different modulators where q is the index of the regulator. The function $f[REG]$ represents the modulation of the conductance by a regulator (such as ions and 2nd messengers) and is dependent on their concentration (see below and *Eqs. 11–14*).

The activation and inactivation functions are modified forms (e.g., Byrne 1980a–c) of the Hodgkin and Huxley (1952) description

$$\frac{dA_{ij}}{dt} = \frac{A_{\infty ij} - A_{ij}}{\tau_{A_{ij}}} \quad (3)$$

$$\frac{dB_{ij}}{dt} = \frac{B_{\infty ij} - B_{ij}}{\tau_{B_{ij}}} \quad (4)$$

where A_∞ and B_∞ are the voltage-dependent steady-state values for activation and inactivation of the conductance j, and τ_A and τ_B are their respective voltage-dependent time constants. The voltage-dependent steady-state values and time constants can also be calculated with the original Hodgkin-Huxley equations (Hodgkin and Huxley 1952), which were used for the simulation of Fig. 5.

Chemical synapses. Currents due to chemical synapses (*Ics*) are calculated with the following equation

$$Ics_{ikl} = \bar{g}cs_{ikl} \cdot Acs_{ikl} \cdot (V_i - Ecs_{ikl}) \quad (5)$$

where $\bar{g}cs$ is the maximal conductance, *Acs* is the time-dependent activation function of the conductance, and *Ecs* is the synaptic reversal potential. The synaptic activation is assumed to act as a second-order system (e.g., Jack and Redman 1971; Rall 1967; Wilson and Bower 1989) of the following form (Coughanowr and Koppel 1975)

$$\frac{d^2Y}{dt^2} = \frac{X - 2\tau \cdot dY/dt - Y}{\tau^2} \quad (6)$$

in which Y is the variable that describes the second-order system,

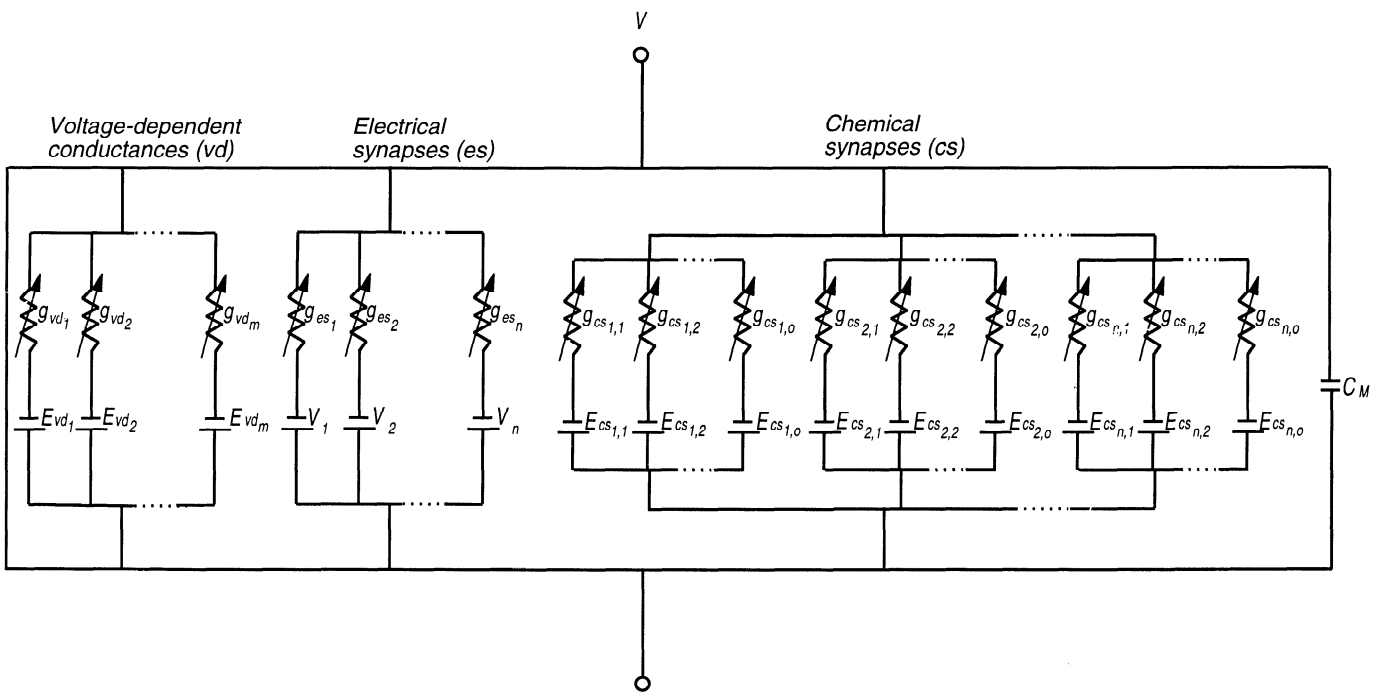

FIG. 1. Electrical circuit equivalent of the membrane model of a neuron in this simulator for neural networks and action potentials (SNNAP). The neuron has a membrane potential V and a membrane capacitance C_M. Currents arise from 3 sources: *1*) m voltage-dependent conductances (g_{vd_1} g_{vd_m}), *2*) n conductances due to electrical synapses ($g_{es_1} - g_{es_n}$), and *3*) mxo time-dependent conductances due to o chemical synapses with each of the n presynaptic neurons ($g_{cs_{1,1}} - g_{es_{n,o}}$). *Evd* and *Ecs* are constants and represent the value of the equilibrium potential for currents due to voltage-dependent conductances and chemical synapses, respectively. $V_1 - V_n$ represent the values of the membrane potential of the coupled cells.

X the forcing function, and τ the time constant. Although the explicit solution of this equation (the alpha function) when X is an impulse is often used to describe the dynamics of synaptic conductance changes (Jack and Redman 1971; Rall 1967; Wilson and Bower 1989), in SNNAP, synaptic conductances are calculated through the numerical solution of this second-order differential equation. This allows for summation of synaptic conductances and for postsynaptic conductances to respond to changes in the duration of the presynaptic action potential (see below). The activation of the synaptic conductance should be a value between 0 and 1, and therefore Y needs to be rescaled by

$$Acs_{ij} = a_{ij} \cdot Y_{ij} \tag{7}$$

where a is a constant. In our system the forcing function X in *Eq. 6* is the synaptic driver, which represents the pool of available transmitter (TP). X equals TP for the duration of the presynaptic spike

$$X_i = \begin{cases} TP_i & \text{during a presynaptic spike} \\ 0 & \text{in the absence of a presynaptic spike} \end{cases} \tag{8}$$

Thus increases (or decreases) in the duration of the presynaptic spike will lead to increases (or decreases) in a postsynaptic current. In addition, TP is not necessarily constant. In a nondepressed synapse TP equals 1, but in a depressed synapse TP equals the level of synaptic depression (SD). SD is calculated with a first-order ODE. SD decays during a presynaptic spike and recovers in the absence of presynaptic spikes

$$\frac{dSD_{ik}}{dt} = \begin{cases} \dfrac{-SD_{ik}}{\tau_{1SD_{ik}}} & \text{during a presynaptic spike} \\ \dfrac{1 - SD_{ik}}{\tau_{2SD_{ik}}} & \text{in the absence of a presynaptic spike} \end{cases} \tag{9}$$

The time constants τ_{1SD}, τ_{2SD} are for decay and recovery, respectively.

Electrical coupling. The contribution of electrical coupling to currents in the membrane is calculated by

$$Ies_{ik} = \bar{g}es_{ik} \cdot (V_i - V_k) \tag{10}$$

where $\bar{g}es$ is the maximal conductance, V_i is the membrane potential of the presynaptic neuron and V_k is the membrane potential of the postsynaptic neuron.

INTRACELLULAR ION POOLS AND SECOND MESSENGERS. Each neuron can have several pools (*ion*), which represent ions whose concentrations are altered by transmembrane fluxes (*Eq. 11*). In addition, a neuron can have several different pools of second messengers (*SM*), which are driven by external inputs (*Eq. 12*). Both *ion* and *SM* can regulate membrane currents (*Eqs. 13* and *14*).

The dynamics of *ion* are described with the following equation

$$\frac{dC_{ion_{iu}}}{dt} = \phi_{iu} \cdot [K_{iu} \cdot (-Ix_{iu}) - C_{ion_{iu}}] \tag{11}$$

where C_{ion} is the variable describing the concentration of the ion u, Ix is the sum of currents that contribute to the concentration of this ion, and ϕ and K are constants.

The dynamics of *SM* are described by

$$\frac{dC_{SM_{is}}}{dt} = \frac{[MOD]_{is} - C_{SM_{is}}}{\tau_{SM_{is}}} \tag{12}$$

where C_{SM} is the concentration of *SM*, *MOD* represents the availability of the external modulator (with a value between 0 and 1 that represents the ratio of the actual concentration of the modulator and the concentration that has the maximal effect), τ_{SM} is the time constant, and s is the index of *SM* in *cell i*.

MODULATION OF CONDUCTANCES BY INTRACELLULAR ION POOLS AND SECOND MESSENGERS. The conductances may be enhanced or attenuated by *ion* or *SM* as described by

$$f[REG] = \begin{cases} \text{gbr} & \text{for enhancement} \\ \dfrac{1}{1 + h \cdot \text{gbr}} & \text{for attenuation} \end{cases} \tag{13}$$

where gbr describes the relation between the concentration of *ion* or *SM* and the level of enhancement or attenuation, and h is a constant. The function gbr is described by

$$\frac{d\text{gbr}}{dt} = \frac{[REG] - \text{gbr}}{\tau_{\text{gbr}}} \tag{14}$$

where $[REG]$ represents the concentration of the regulator (C_{ion} or C_{SM}, see *Eqs. 11* and *12*) and τ_{gbr} is the time constant.

Hardware and software

SNNAP was programmed on SPARCstation 2, with the use of the C programming language and Xlib. The time of execution is correlated with the complexity of the system that is modeled. For example, the addition of a single voltage-dependent conductance or a chemical synapse increased the CPU time required for a single itteration by 1.3×10^{-4} and 1.4×10^{-5}, respectively. The simulations illustrated in this paper required between 30 s and 2 h to run on a 40-MHz SPARCstation 2.

Input/output controls

A list of optional equations for calculating various state and intermediate variables is available. For example, there are two optional sets of functions to calculate the activation and inactivation of voltage-dependent conductances: through rate constants (e.g., Hodgkin and Huxley 1952) or through time constants (e.g., Byrne 1980a–c). Values to any of the parameters or constants, relevant to each variable, are assigned independently. The list of equations and associated parameters and constants in addition to the operational information (e.g., the duration of the simulation and type of output display) are passed to the program through a number of modular ASCII files. These files can be modified by commonly available text editors that use conventional (i.e., characters based) interfaces of by an editor incorporated into SNNAP that uses a graphical interface. These modules are organized hierarchically (Fig. 2). The module *simulation* is at the top of the hierarchy and directs all other relevant modules. The other major modules are *1*) *network*, which specifies which neurons are included in the network and the type and pattern of their synaptic connections; *2*) *neuron*, which specifies voltage-dependent conductances, pools of ions, and modulators; and *3*) *voltage-dependent conductances*, which specifies the maximal conductance, the reversal potential, and the names of the modules dealing with the voltage-dependent activation and inactivation and with the modulation of the conductance. The modules *electrical synapse*, *chemical synapse*, *ion pool*, *SM* (2nd messenger) *pool*, *modulation by ion*, *modulation by SM*, *activation*, and *inactivation* all specify the relevant equations and parameters for each variable. Other modules serve to describe operational information for the specific simulation including a module (*treatments*) that describes the timing of external currents and modulatory stimuli.

SNNAP's output options include on-line display of any variable versus time and the ability to write the simulation's results into an output file, for further analysis.

Integration method and parameters

For reason of simplicity, the Euler method was used to integrate numerically the set of differential equations (for discussion of integration routines see Press et al. 1992). To minimize possible errors in simulations that might arise if the step size was too large, we first made a trial simulation with a comparatively large step

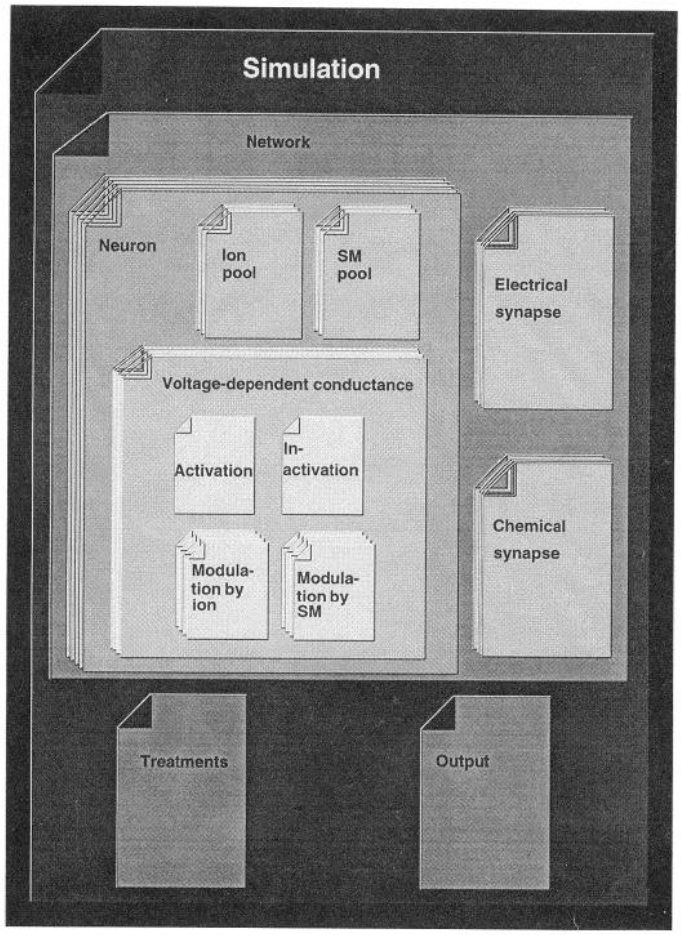

FIG. 2. Equations, parameters, initial conditions, and operational options for a specific simulation are passed to the program through a set of modular files, organized in a hierarchical way. The module *Simulation*, at the top of the hierarchy, specifies all relevant modules. Under *Simulation* there are 3 modules: *Network*, which specifies the connection between cells; *Treatments*, which specifies the types of treatments that the network will receive; and *Output*, which specifies the variables to be included in the output file or output graph. The modules included in *Network* are *Neuron*, which specifies the chemical- and voltage-dependent processes in the individual neurons and the modules, *Electrical synapse* and *Chemical synapse*, which specify the equations and parameters describing the interconnections among neurons. The modules nested in *Neuron* are *Ion pool* and *SM pool* for choosing the equations and parameters for calculating the dynamics of different ions and 2nd messengers, respectively. *Neuron* also includes the module *Voltage-dependent conductance*. The modules *Activation, Inactivation, Modulation by ion*, and *Modulation by SM* are all nested in *Voltage-dependent conductance* and specify the set of equations and parameters required for calculating the activation and inactivation functions of specific conductances and the modulation of conductances by ions and 2nd messengers.

size and then reran the simulation with progressively smaller step sizes. We continued to reduce the step size to a point where further reduction did not change the results. Values for acceptable step sizes ranged between 0.1 and 0.01 ms.

The parameters for the intrinsic properties of neurons were either taken from the literature or were adjusted to match a given pattern of neuronal activity. Parameters for connectivity and for neural modulation were chosen to match physiological patterns.

RESULTS

We first simulated the electrical properties of several types of neurons by incorporating different combinations of specific voltage-dependent conductances. Next we simulated small networks, features of synaptic plasticity, and the modulation of the voltage-dependent conductances. Finally, we simulated a more complex network and its modulation.

Intrinsic properties of individual neurons

The nervous system of both vertebrates and invertebrates includes various types of neurons with distinctive intrinsic biophysical properties. By adjusting the types of voltage-dependent conductances as well as the parameters in the equations describing voltage-dependent conductances and the leakage conductance, neurons with diverse firing properties were simulated. Figure 3 illustrates several examples of these neurons (see also Table 1). A tonic firing neuron was simulated by constructing a neuron with only Na^+, K^+, and leakage conductances. The properties of both the Na^+ and K^+ conductances were derived from the ink motor neuron of *Aplysia* (Byrne 1980a–c). The K^+ conductance in these cells, as in many other neurons, exhibits inactivation. In this cell a depolarizing current pulse led to continuous firing of the simulated neuron (Fig. 3*A*). A pacemaker neuron was simulated by simply changing the equilibrium potential of the leakage current to a more depolarized value (Fig. 3*B*). We also simulated the physiological properties of the ink motor neuron of *Aplysia* (Byrne 1980a–c). This modeled neuron included Na^+, Ca^{2+}, K^+, and transient K^+ ($I_{K,A}$) conductances. In response to an intracellular depolarization, $I_{K,A}$ was activated, which initially prevented the cell from firing. After ~1 s (during which $I_{K,A}$ became inactivated), the neuron began to fire (Fig. 3*C*). A neuron that exhibited an adaptive response was simulated with the use of the physiological properties of the sensory neurons of *Aplysia* (Fig. 3*D*) (Baxter and Byrne 1990; Canavier et al. 1991; White et al. 1991, 1993). The conductance underlying the adaptive response is a novel low-threshold noninactivating K^+ conductance (the S-current, $I_{K,S}$) (Baxter and Byrne 1990; Klein et al. 1982). Intracellular depolarization elicited an early burst of spikes, but firing ceased as $I_{K,S}$ became activated and opposed the effectiveness of the depolarizing pulse to fire the cell. A plateau potential–type response was simulated by including an slowly inactivating inward current (I_{dep}) and a slowly activating, noninactivating outward current (I_{hyp}) (Fig. 3*E*). I_{dep} remained active even after termination of the intracellular depolarizing current pulse thereby allowing the cell to continue firing until I_{hyp} was activated sufficiently to prevent firing. A neuron that exhibited postinhibitory rebound (Fig. 3*F*) was simulated by the addition of noninactivating K^+ conductance (as in Fig. 3*D*) to a spontaneously active cell (as in Fig. 3*B*).

Network simulations

Because the organization of individual neurons into functional systems is through synapses, our next goal was to simulate simple networks interconnected through chemical or electrical synapses (Fig. 4, *A* and *B*; see also Table 2).

CHEMICAL SYNAPSES. *Feed-forward excitatory and inhibitory connections and summation of postsynaptic potentials*

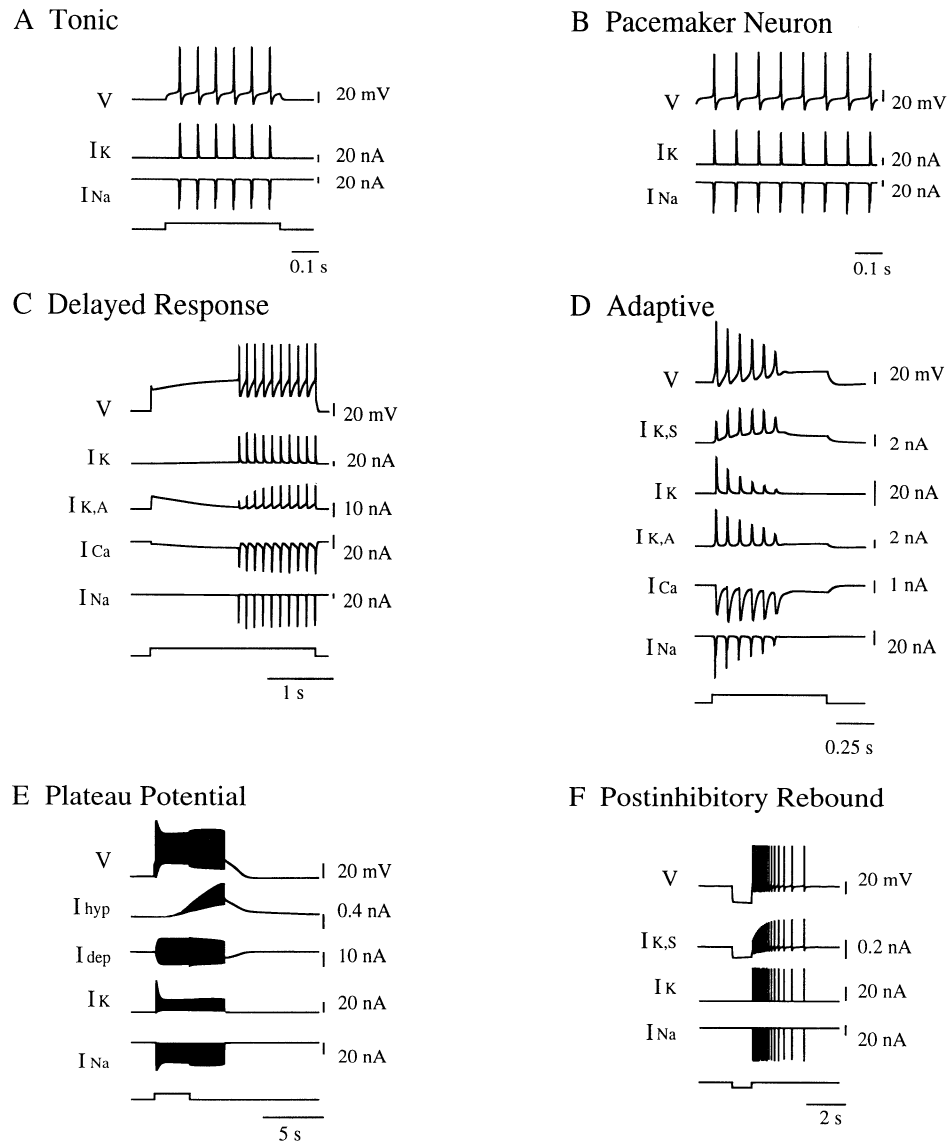

FIG. 3. Intrinsic properties of individual neurons. *A*: tonic firing. The neuron was simulated with only Na^+, K^+, and leakage conductances (Table 1A). A depolarizing current pulse of 2.5 nA led to continuous firing of the simulated neuron. Action potentials were due to a voltage-dependent increase in I_{Na} followed by a delayed increase in I_K. *B*: pacemaker neuron. Changing the equilibrium potential of the leakage current of the neuron, illustrated in *A*, to a more depolarized value (Table 1B) resulted in spontaneous activity. *C*: delayed response. The modeled neuron included the currents I_{Na}, I_{Ca}, and I_K, and the transient K^+ current ($I_{K,A}$). Parameters for this neuron were taken from the model of the ink motor neuron (Byrne 1980a–c) and are provided in Table 1C. In response to the depolarization produced by an intracellular current pulse of 22.3 nA, $I_{K,A}$ was activated. $I_{K,A}$ initially prevented the cell from firing, but as $I_{K,A}$ inactivated the neuron reached threshold and fired a burst of spikes. *D*: adaptive. This neuron was simulated on the basis of the physiological properties of sensory neurons of *Aplysia* (Table 1D). The conductance underlying the adaptive response was a noninactivating K^+ conductance ($g_{K,S}$). An intracellular depolarizing current pulse of 1.5 nA elicited an early burst of spikes. Firing ceased as $I_{K,S}$ became activated and opposed the effectiveness of the depolarizing current pulse. *E*: plateau potential. A plateau potential–type response was simulated with a slowly inactivating inward current (I_{dep}) and a slowly activating and noninactivating outward current (I_{hyp}). Parameters for each current are provided in Table 1E. I_{dep} remained active even after termination of the intracellular depolarizing current pulse (3.0 nA). Thus the cell continued to fire until I_{hyp} was activated sufficiently to prevent firing. *F*: postinhibitory rebound. Addition of a noninactivating K^+ conductance (such as in the neuron in *D*) to a spontaneously active cell (such as the neuron in *B*) produced a cell that exhibited postinhibitory rebound (elicited by a hyperpolarizing current of 0.3 nA). Parameters are provided in Table 1F.

(*PSPs*). Figure 4*A1* illustrates the results from a simulation of a three-cell network. Chemical synapses were formed between the presynaptic *cell A* and the postsynaptic *cells B* and *C*. A single spike in *cell A*, which was elicited by a brief depolarizing current pulse, produced a unitary excitatory PSP (EPSP) in *cell B* and unitary inhibitory PSP (IPSP) in *cell C*. A longer depolarizing pulse elicited a series of three spikes in *cell A*, which produced summating EPSPs in *cell B* and IPSPs in *cell C*. Note that the magnitudes of individual components of the PSPs do not summate linearly because of a decrease in the driving potential of the chemical PSPs (see *Eq. 5*).

TABLE 1. *Parameters for intrinsic properties of neurons*

Neuron	C_M, μF	Conductance	E, mV	$\bar{g}$, μS	p	A/B	A_∞/B_∞ B_{min}	h	s	p	τ_A/τ_B, s τ_{max}	τ_{min}	h	s	p
A. Tonic/															
B. Pacemaker	0.0013	Na	76.6	7.5	3	*A*		−18.1	4.8	1	0.0015	0.00045	−8.7	1.85	1
						B	0.0	−27.5	9.2	1	0.01	0.0024	−15.2	3.5	1
		K	−70.0	12.0	1	*A*		−2.4	8.8	1	0.01	0.027	−0.0004	11.7	1
													−27.0	−11.2	1
						B	0.15	8.4	1.5	2	0.2	0.02	−0.0004	8.3	1
		Leak	−39.8/−30.0	0.25											
C. Delayed															
response	0.001	Na	67.0	7.8	3	*A*		−18.1	4.8	1	0.0014	0.00039	−8.7	1.9	1
						B	0.15	−27.5	9.2	1	0.0237	0.00571	−15.2	3.5	1
		Ca	87.0	1.2	1	*A*		−1.3	10.8	1	0.0087	0.001	42.8	21.8	2
						B	0.24	−16.3	7.9	2	0.3726	0.067	−40.1	33.3	1
		K	−75.0	19.8	1	*A*		3.9	6.6	1	0.145	0	−0.4	12.6	1
													−23.0	−13.3	1
						B	0.0	8.0	12.8	3	1.066	0.02	−8.0	7.4	1
		K, A	−65.0	7.0	2	*A*		−14.2	22.8	1	0.01	0.0038	−17.8	3.5	2
						B	0.0	−54.2	6.5	1	0.3074	0.049	19.7	11.0	3
		Leak	−75.0	0.5											
D. Adaptive	0.001	Na	70.0	8.0	3	*A*		−18.1	8.8	1	0.0020	0.00056	−9.0	7.0	1
						B	0.0	−37.0	3.2	1	0.01	0.0028	−9.0	7.0	1
		Ca	60.0	0.15	3	*A*		−20.0	10.8	1	0.05	0.006	−20.0	21.8	1
						B	0.75	−16.3	7.9	1	0.3706	0.278	−40.1	33.3	1
		K	−70.0	4.2	3	*A*		3.7	9.5	1	0.028	0.0028	22.0	17.5	1
						B	0.0	−22.9	12.4	1	0.46	0.046	5.7	1.9	1
		K, A	−70.0	0.45	2	*A*		−20.7	26.0	1	0.015	0.005	−33.8	2.9	1
						B	0.0	−49.3	23.3	1	0.14	0.0462	−30.0	5.8	1
		K, S	−70.0	0.45	1	*A*		21.2	19.7	1	0.255	0.0612	−15.0	10.0	1
													−46.0	−6.5	1
		Leak	−24.1	0.033											
E. Plateau															
potential	0.00013	Na	53.7	2.3	3	*A*		−40.0	4.8	1	0.00014	0.00004	−30.65	1.85	1
						B	0.0	−49.4	9.15	1	0.0012	0.00029	−37.1	3.508	1
		Depolarized	−30.0	1.0	3	*A*		−57.1	12.5	1	0.23	0.064	−36.83	7.0	1
						B	0.0	−64.8	3.2	1	55.01	15.4	−36.8	7.0	1
		K	−86.9	19.0	4	*A*		−29.4	8.8	1	0.0027	0.0002	−21.9	11.72	1
													−48.9	−11.2	1
						B	0.148	−14.5	1.47	2	0.02	0.002	−21.9	8.26	1
		Hyperpolarized	−86.9	10.2	3	*A*		−34.8	0.9	1	23.9	6.7	−36.8	7.5	1
		Leak	−73.0	0.18											
F. Postinhibitory															
rebound	0.0002	Na	55.6	2.0	3	*A*		−33.1	4.8	1	0.00014	0.00004	−23.7	1.85	1
						B	0.0	−42.5	9.15	1	0.0012	0.00029	−30.2	3.508	1
		K	−62.0	13.0	4	*A*		−17.4	8.8	1	0.0028	0.0002	−15.0	11.72	1
													−42.0	−11.2	1
						B	0.148	−6.6	1.47	2	0.02	0.002	−15.0	8.26	1
		K, S	−65.0	0.028	1	*A*		−32.4	9.1	1	0.95	0.23	−15.0	10.0	1
													−46.0	−6.5	1
		Leak	−39.0	0.009											

E is the reversal potential, $\bar{g}$ the maximal conductance, and p the exponent for the activation function. A and B are the activation and inactivation terms, respectively. A_∞ and B_∞ are the steady-state values for A and B, respectively, and were calculated by

$$A_\infty = \{1 + \exp[(V - h)/s]\}^{-1} \qquad B_\infty = (1 - B_{min}) \times \{1 + \exp[(h - V)/s]\}^{-p} + B_{min}$$

where V is membrane potential, h is the shift parameter, s is the shape parameter, and B_{min} is the minimal value of B. τ_A and τ_B are the time constants for A and B, respectively, and were calculated by

$$\tau_A = \frac{\tau_{max} - \tau_{min}}{\left[1 + \exp\left(\frac{V - h_1}{s_1}\right)\right]^{p_1} \cdot \left[1 + \exp\left(\frac{V - h_2}{s_2}\right)\right]^{p_2}} + \tau_{min} \qquad \tau_B = \frac{\tau_{max} - \tau_{min}}{\left[1 + \exp\left(\frac{V - h}{s}\right)\right]^{p}} + \tau_{min}$$

where V is the membrane potential, h is the shift parameter, and s is the shape parameter. The subscripts of h, s, and p are for a double exponential model. The table shows parameters for 1st exponent and 2nd exponent in the 1st and 2nd row, respectively. One row indicates a single exponent model (where $p_2 = 0$).

Network with feedback chemical synapses. Patterns of rhythmic neural activity are common features of the nervous system. It has been suggested that rhythmic patterns can be produced when a tonicly active neuron excites a second neuron, which in turn, inhibits the first (e.g., Milton et al. 1990). We constructed such a network (Fig. 4*A2*) in which *cell A* made an excitatory connection to *cell B*, and *cell B* made an inhibitory connection to *cell A*. The injection of constant depolarizing current into *cell A* led to the initiation of spikes in *cell A* and excitation of *cell B*. The EPSPs in *cell B* summated until threshold was reached for a spike in *cell B*. The spike in *cell B* led to an IPSP in *cell A* and thus a transient cessation of firing in *cell A*. After *cell A* recovered from inhibition, the cycle was reinitiated.

ELECTRICAL COUPLING. Figure 4*B* illustrates a network that was constructed such that *cells A* and *B* were electrically coupled to *cell C*. Current was injected to *cells A* and

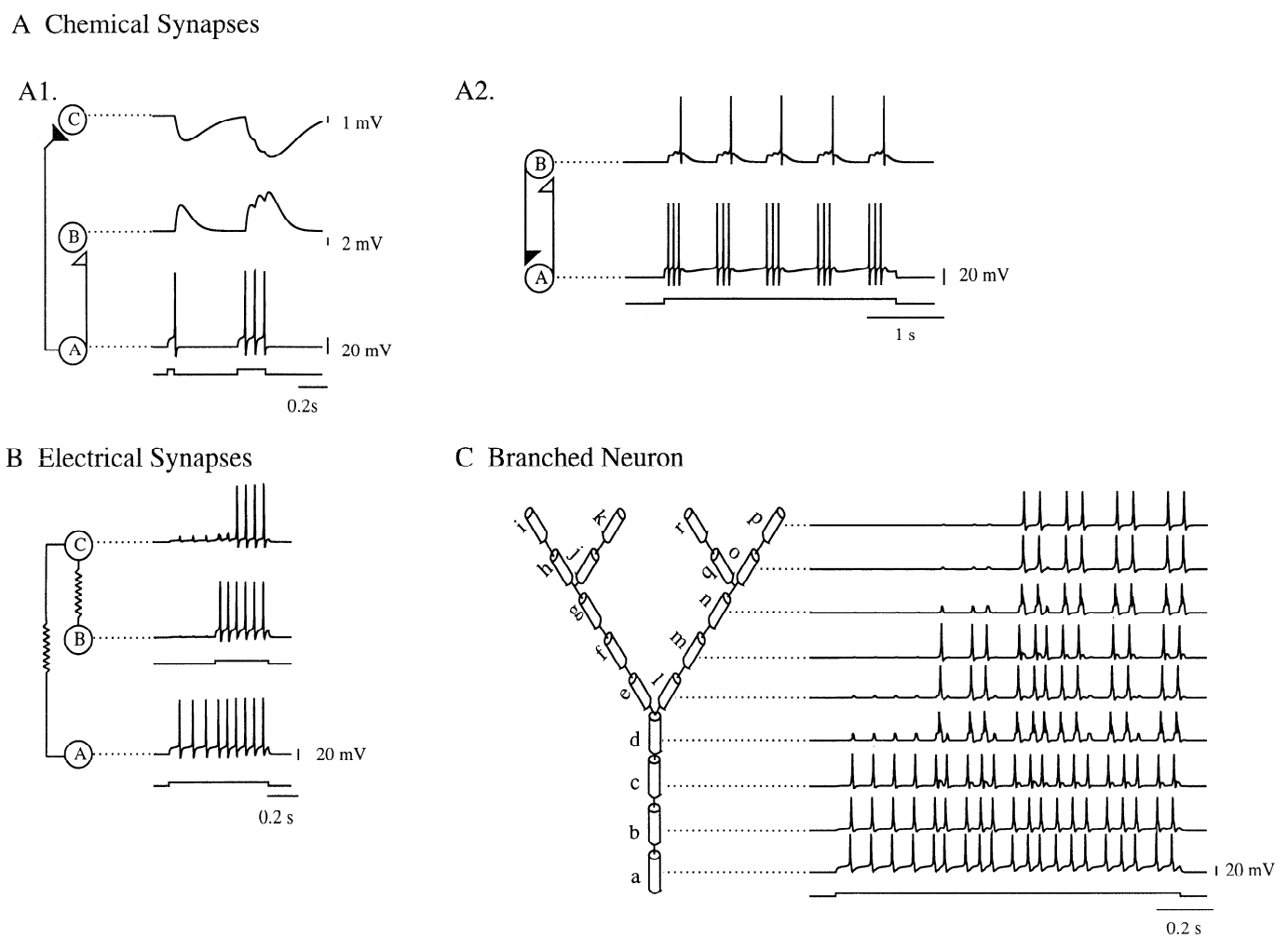

FIG. 4. Network and multicompartmental simulations. *A*: chemical synapses. *A1*: a network of 3 cells was simulated in which chemical synapses were formed between the presynaptic *cell A* and the postsynaptic *cells B* and *C* (Table 2A). The excitatory connection between *cells A* and *B* is indicated by an open triangle and the inhibitory connection by a filled triangle. A single spike in *cell A* elicited by a 3-nA depolarizing current pulse (timing of depolarizing current is indicated by a square pulse at the bottom of the figure) produced a unitary excitatory postsynaptic potential (EPSP) in *cell B* and unitary inhibitory postsynaptic potential (IPSP) in *cell C*. A longer depolarizing pulse elicited a series of 3 spikes in *cell A*, which produced summating EPSPs in *cell B* and IPSPs in *cell C*. *A2*: a 2-cell network (Table 2B) was simulated that generated a cyclical pattern of activity. *Cell A* had an excitatory connection (open triangle) to *cell B*, and *cell B* had an inhibitory connection (filled triangle) to *cell A*. The injection of a 2.5-nA depolarizing current pulse to *cell A* led to the initiation of spikes in *cell A* and to the excitation of *cell B*. The EPSPs in *cell B* summated until *cell B* fired a single spike that led to the inhibition of *cell A*. As *cell A* recovered from inhibition, the cycle was reinitiated. *B*: electrical coupling. A network was constructed in which the *cells A* and *B* were electrically coupled to *cell C*. The coupling conductance was 0.07 μS. A depolarizing current pulse of 3.0 nA was injected into *cells A* and *B* at different times (timing is indicated by a square pulse at the bottom of the traces showing the membrane potentials). When only *cell A* was spiking, small subthreshold PSPs in *cell C* were produced. After activation of both *cells A* and *B*, the electrical PSPs summated, and spikes were initiated in *cell C*. *C*: branched neuron. A branched neuron consisting of 18 compartments (*a–r*) was simulated. The coupling conductance between each pair of adjacent compartments was set to 0.195 μS. Injection of a 3.9-nA depolarizing current pulse into *compartment a* initially induced spikes in *compartments a, b,* and *c* and smaller depolarizations in more distant compartments of the neuron. As *compartments d–r* became more depolarized, spikes in *compartments a–c* were more effective in eliciting spikes in the more distal compartments. The intrinsic properties of all the neurons (or compartments) shown in this figure were simulated as the neuron described in Fig. 3*A* and Table 1A. Parameters for connectivity are provided in Table 2.

B at different times. When only *cell A* was spiking, small subthreshold electrical PSPs were observed in *cell C*. With activation of both *cells A* and *B*, the electrical PSPs summated, and spikes were initiated in *cell C*.

Branched neuron

Compartmental modeling, derived from linear cable theory (e.g., Rall 1989), is usually used to simulate the flow of currents in time and space within a dendritic tree (e.g., Segev 1992; Segev et al. 1989). With this method the neuron is modeled as a system of electrically coupled membrane cylinders. Although SNNAP is not capable of dealing with large-scale compartmental models, its electrical coupling features can be used to simulate the properties of simple branched neurons. Figure 4*C* summarizes the results of a simulation of a branched neuron that was divided into 18 compartments. Each compartment had the same dimen-

TABLE 2. *Parameters for connectivity*

	Related Figure	Pre	Post	E, mV	$\bar{g}$, μS	τ, s	a
A	4*A1*	*A*	*B*	−37.0	0.25	0.08	73.2
			C	−42.0	0.08	0.08	73.2
B	4*A2*	*A*	*B*	−20.0	0.225	0.04	36.6
		B	*A*	−42.0	0.08	0.08	73.2
C	6*B*	*A*	*B*	7.0	0.097	0.001	0.912
D	7	*A*	*B*	−3.0	0.25	0.001	0.912

Pre and Post, presynaptic and postsynaptic cells, respectively. E is the reversal potential, $\bar{g}$ the maximal conductance, τ the time constant, and a the scaling factor for synaptic conductance (see *Eq. 7*).

sions and electrical properties. A depolarizing current pulse was applied to one part of the branched neuron (*compartment a*). At first, only *compartments b* and *c* initiate spikes, whereas little depolarization was seen in more distant compartments of the neuron. Gradually, distant compartments (e.g., *i*, *k*, *r*, and *p*) began to initiate spikes as well.

Modulation of membrane currents and synaptic conductances

Modulation of membrane channels and release mechanisms are believed to be important mechanisms underlying many aspects of neural function, such as motor activity and processes of learning and memory (Byrne 1987; Clarac et al. 1992; Hultborn and Kiehn 1992; Kandel 1985; Kupfermann 1991; Shepherd 1988). SNNAP incorporates several different ways to simulate modulation of voltage-dependent and synaptic conductances. The properties of voltage-dependent conductances may be modulated by changes in the concentration of internal ions or application of modulatory agents. Synaptic conductances may be modulated by changes in the duration of the presynaptic spike. SNNAP also allows for the simulation of synaptic depression.

CALCIUM-DEPENDENT MODULATION OF MEMBRANE CURRENTS. On the basis of the model proposed by Epstein and Marder (1990), a bursting neuron (Fig. 5) was simulated, which included the voltage-dependent Na^+ and K^+ conductances, a Ca^{2+}-inactivated Ca^{2+} conductance (g_{Ca}), and a Ca^{2+}-activated K^+ conductance ($g_{K,Ca}$). The model also included a Ca^{2+} pool. An initial depolarization due to I_{Ca} led to a burst of Na^+-dependent spikes. The spikes led to accumulation of Ca^{2+} during the burst. Consequently, $I_{K,Ca}$ was activated and I_{Ca} was deactivated, both of which led to the termination of the burst. During the postburst hyperpolarization, Ca^{2+} levels were decreased, $I_{K,Ca}$ deactivated, and another burst of spikes was initiated.

SECOND-MESSENGER MODULATION OF MEMBRANE CURRENTS. Plasticity at the connection between sensory neurons and the follower cells in *Aplysia* has been used as a model system in which to study the neural basis of simple forms of learning such as sensitization (Byrne 1987; Byrne et al. 1993; Carew and Sahley 1986; Kandel and Schwartz 1982). Serotonergic modulation of sensory neurons, which contribute to sensitization, both enhances excitability and increases the duration of action potentials. These two actions of serotonin (5-HT) were simulated.

Excitability. The noninactivating K^+ conductance ($g_{K,S}$) of the sensory neuron is modulated by a 5-HT–induced increase in the levels of the second-messenger adenosine 3′,5′-cyclic monophosphate (cAMP) (Baxter and Byrne 1989; Klein et al. 1982). As a first step in simulating this example of plasticity, we incorporated a slowly activating and noninactivating K^+ conductance that was regulated by the concentration of cAMP. The responses of a pair of simulated sensory neurons to two successive intracellular depolarizing pulses are illustrated in Fig. 6 (see also Table 3). For the control sensory neuron (Fig. 6*A1*), each of the two successive pulses elicited two spikes. For the experimented sensory neuron (Fig. 6*A2*), application of 5-HT was simulated after the first pulse. Note that the 5-HT led to a depolarization of the resting potential. This was due to the 5-HT–induced elevation of cAMP levels, which led to a decrease in the steady-state level of $I_{K,S}$. A second effect of the simulated application of 5-HT was enhanced excitability. Note that the second pulse in the presence of 5-HT led to a greater number of action potentials.

Spike width. Spike broadening is one way to increase synaptic strength of sensory neurons in *Aplysia* (Byrne et al. 1990; Gingrich and Byrne 1987; Hochner et al. 1986; Klein and Kandel 1978; Sugita et al. 1992). We simulated a two-cell network in which the sensory *cell A* had an excitatory connection onto follower *cell B* (Fig. 6*B*). Simulating the application of 5-HT led to an increase in the simulated levels of protein kinase C (PKC), which in turn gradually reduced a delayed K^+ current (I_K; Fig. 6*B2*). Because of the decrease of outward current, the spikes in *A* are broadened (Fig. 6*B3*). The broadened spikes, in turn, led to enhanced transmitter release and increased the synaptic conductance in *cell B*. As the presynaptic spike broadened, the EPSP was enhanced sufficiently to elicit a spike in *cell B*. Note that the network was affected even after removing 5-HT, because of

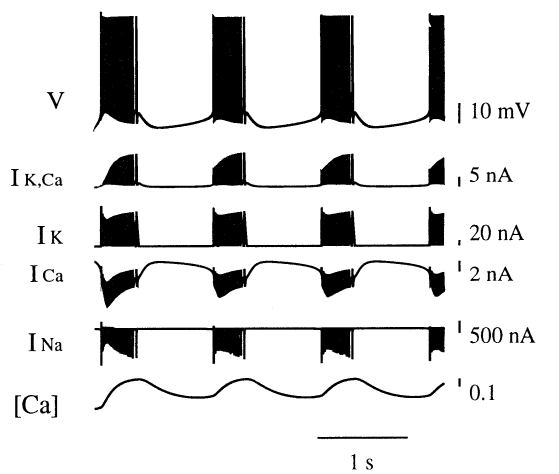

FIG. 5. Simulation of an endogenous bursting neuron and Ca^{2+}-dependent modulation of membrane currents. The neuron included the voltage-dependent conductances g_{Na} and g_K, a Ca^{2+}-inactivated Ca^{2+} conductance (g_{Ca}), a Ca^{2+}-activated K^+ conductance ($g_{K,Ca}$), and an intracellular Ca^{2+} pool (parameters taken from Epstein and Marder 1990). An initial depolarization due to I_{Ca} led to a burst of Na^+-dependent action potentials. The action potentials led to accumulation of Ca^{2+}. The burst of spikes was terminated due to both the activation of $I_{K,Ca}$ and the inactivation of I_{Ca}. During the interburst interval, Ca^{2+} levels were decreased, $I_{K,Ca}$ deactivated and I_{Ca} deinactivated, both of which allowed for the initiation of another burst of spikes.

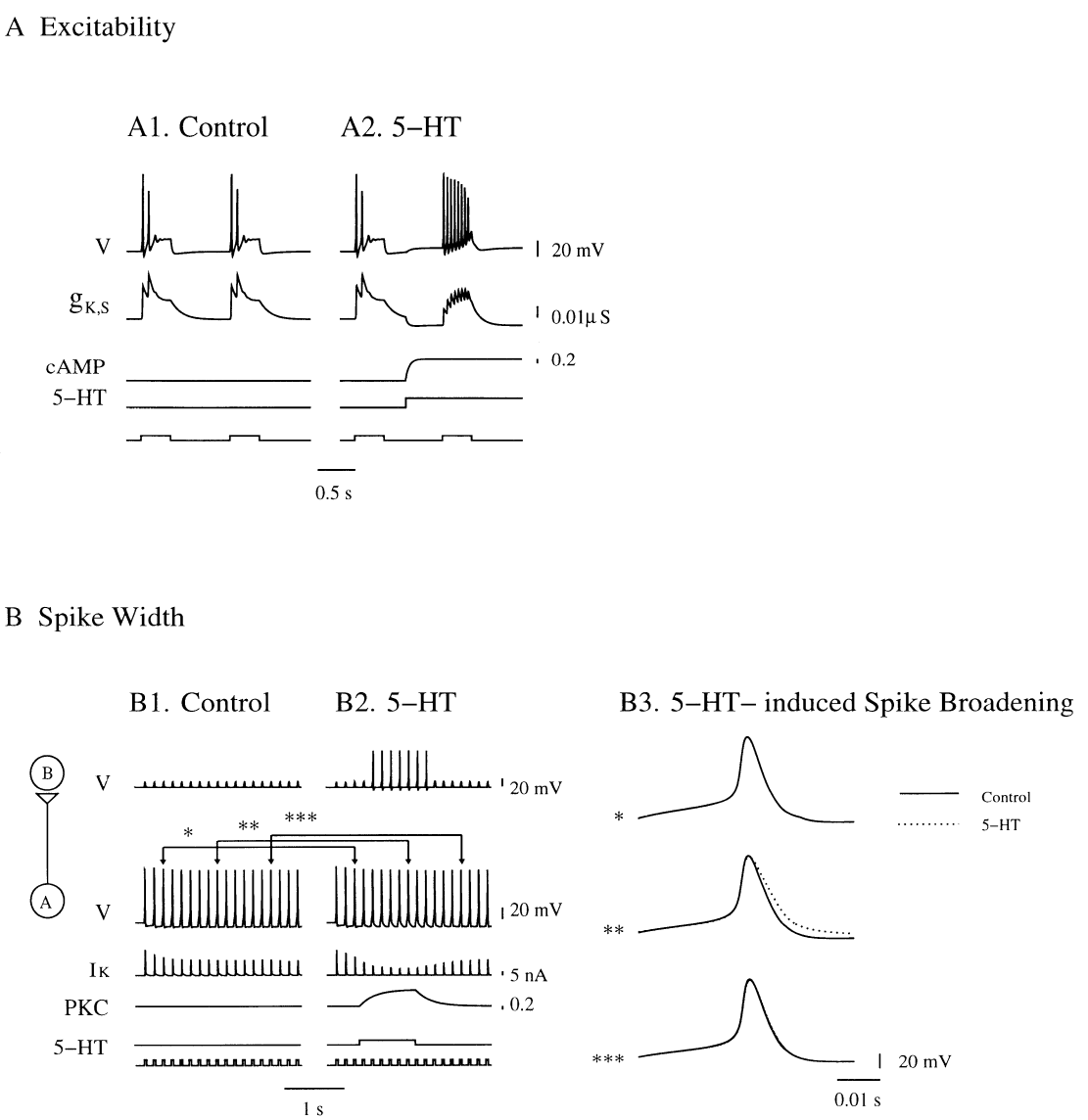

FIG. 6. Second-messenger modulation of excitability and spike width. *A*: changing the excitability of a sensory neuron of *Aplysia* by modulating $I_{K,S}$. The neuron (simulated as the neuron in Fig. 3*D*, Table 1D) included a noninactivating K^+ conductance ($I_{K,S}$) that was modulated by serotonin (5-HT; parameters for modulation are provided in Table 3A). Two depolarizing current pulses were applied during both the control (*A1*) and experimental (*A2*) simulations. The application of 5-HT led to an increase in the levels of adenosine 3′,5′-cyclic monophosphate (cAMP), which in turn decreased the maximum conductance of $I_{K,S}$. Reducing $g_{K,S}$ depolarized the resting potential and increased the number of action potentials elicited by the 2nd pulse. *B*: changing the spike width of a neuron by modulating I_K. A 2-cell network (Table 2C) with an excitatory connection between the sensory *neuron A* (Table 1D) and the follower *cell B* (Table 1A) was constructed. Identical trains of 40-ms duration depolarizing current pulses were applied every 0.1 s. In the control simulation (*B1*) stable EPSPs were produced in *cell B* by the spikes in *cell A*. These EPSPs were subthreshold for initiating spikes in *cell B*. Application of 5-HT to the presynaptic neuron (*A*) in the experimental simulation (*B2*) led to a slow increase in the activation of protein kinase C (PKC), which in turn gradually reduced g_K. This decrease led to an increase in the duration of the presynaptic action potential (parameters for modulatory effects are provided in Table 3B) and enhancement of transmitter release. As the synaptic conductance in *cell B* was enhanced, the EPSP became sufficiently large to reach threshold and fire an action potential in *cell B*. *B3* illustrates the 5-HT–induced increase in the duration of the action potential in *cell A*.

TABLE 3. *Parameters for neural modulation*

	Related Figure	τ_{SM}, s	τ_{gbs}, s	b
A	6*A*	0.05	0.0001	1
B	6*B*	0.25	0.001	2

τ_{SM} and τ_{gbs} are time constants, and b is a shape parameter (see *Eqs. 12–14*).

the slow decay in the concentration of PKC. In the control simulation (Fig. 6*B1*) the magnitudes of EPSPs remained stable for all spikes in *cell A*.

SYNAPTIC DEPRESSION. Synaptic depression was simulated with a simple depletion-type model. Figure 7 illustrates a two-cell network with an excitatory connection between *cells A* and *B*. An intracellular depolarizing current pulse led to the initiation of three action potentials in *cell A*. With

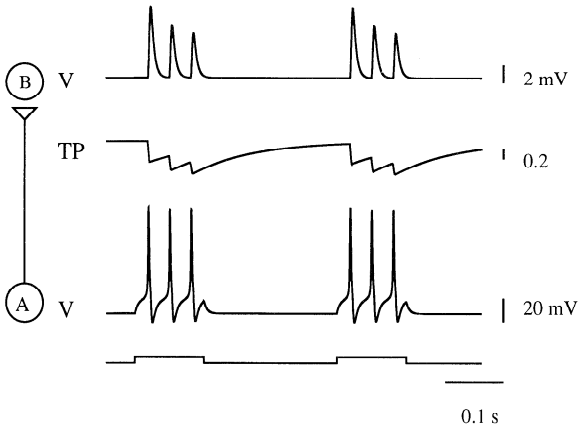

FIG. 7. Synaptic depression. A 2-cell network (the parameters for simulating the intrinsic properties of each neuron are provided in Table 1*A*) was constructed with an excitatory connection between *cells A* and *B* (Table 2*D*). A depolarizing current pulse of 3.0 nA was injected into *cell A*, which initiated 3 action potentials. With each action potential, the PSP elicited in *cell B* was smaller because of the decrease in the pool of available transmitter (*TP*). After 230 ms, a 2nd depolarizing current pulse of the same magnitude was injected into *cell A*. The 1st action potential in *cell A* elicited a PSP of the same magnitude as the 1st spike of previous depolarization, because *TP* had returned to its initial value. Time constants for decay and recovery of transmitter availability were 6 and 100 ms, respectively.

each action potential, the PSP in *cell B* was smaller because of the decrease in the level of available transmitter (*TP*). In the interval between the two current pulses, the PSPs recovered because *TP* returned to its initial value.

Simulating the activity and the modulation of a central pattern generator (CPG)

We have also begun to use SNNAP to simulate features of a more complex neural network. We were guided by recent identification of components of a CPG in the buccal ganglia of *Aplysia*, which includes *neurons B31, B35, B51,* and *B52* (Plummer and Kirk 1990; Susswein and Byrne 1988). Using multifunctional *neuron B4* as a monitor of activity in the buccal ganglia, Susswein and Byrne (1988; see also Baxter and Byrne 1991) identified a pattern of activity, which they termed Pattern 2. Pattern 2 is characterized by the simultaneous depolarization of the nonspiking *neuron B31* and excitation in *neurons B35* and *B52*. This activity in *B31, B35,* and *B52* is followed by a powerful inhibition that coincides with a burst of action potentials in *neurons B4* and *B51*. Injection of a brief depolarizing current pulse into *B31* elicits a single cycle of this pattern, whereas injection of constant depolarizing current elicits multiple cycles.

To examine whether these elements are sufficient for generating the rhythmic activity in the buccal ganglia, we first simulated a network that consisted of *B31, B35, B51, B52,* and *B4*. The synaptic connections among these neurons are illustrated in Fig. 8 (see also Table 4) and are based on the experimental data of Plummer and Kirk (1990) and Baxter and Byrne (1991). The process of simulating the network consisted of three steps. First, we simulated the characteristic firing properties of the individual neurons. Second, we simulated the features of the synaptic connections. Third, we incorporated all the components into the network. At each step, parameters were adjusted to match experimental data and then fixed, to ensure that the chosen parameters reflected the experimental data and were not biased by the attempts to simulate the neural pattern.

The first attempt to simulate the rhythmic neural activity of Pattern 2 with only neurons *B31, B32, B51, B52,* and *B4* failed (Fig. 8*A*). Injection of a brief depolarizing current into *B31* elicited a regenerative depolarization of *B31* and a burst of spikes in *B35,* but no activity in *B4* or *B51*. This indicates that one or more additional unidentified elements of the CPG may contribute to the generation of the pattern. To examine this possibility we incorporated an additional neuron (*neuron I*) into the network. From examination of the failed attempt to generate the pattern of activity (Fig. 8*A*), we predicated that the properties of *neuron I* should include an intrinsic regenerative response to depolarization, and it should receive excitatory input from *B35,* provide feedback inhibition to *B31* and *B35,* and provide excitation to *B4* and *B51*. With the addition of *neuron I,* a single cycle of patterned activity, which was similar to Pattern 2, was initiated by injecting a brief depolarizing current pulse into the nonspiking *neuron B31* (Fig. 8*B*). In the model the depolarization of *B31* led to a depolarization of the electrically coupled *cell B35*. The resultant spikes in *B35* led to summating EPSPs in *cell I*. When the EPSPs reached threshold, the spikes in *neuron I* led to strong inhibition of *B31, B35,* and *B52* and excitation of *B51* and *B4*. Because of the regenerative response of *cell I,* it continued to fire for a few more seconds. [Subsequent experimental work (Hurwitz et al. 1993; Baxter and Byrne, unpublished observations) has identified a neuron in the buccal ganglia, *B64,* whose properties and synaptic connections are similar to those predicted by the model of the buccal CPG.]

With simulations such as these, it is possible to investigate how specific biophysical properties of a single neuron contribute to the activity of the network. In addition, it is possible to examine how modulation of membrane currents, or synaptic strengths, can effect the output of the network. For example, we have examined how a modulatory agent that alters the properties of *neuron I* might effect the activity of the CPG (Fig. 9). Injection of a constant depolarizing pulse elicited sustained patterned activity in the network. We simulated the application of an agent that modulates the slow inward current of *neuron I*. As the conductance of the slow inward current of *neuron I* was gradually reduced, more time was needed for *cell I* to reach threshold for firing, which in turn, resulted in a lower frequency of the pattern and in a reduction in the number of action potentials during each burst.

DISCUSSION

There is an increasing awareness that mathematical modeling and simulations are necessary tools not only for theoreticians but also for experimentalists who wish to explore the properties of complex neural systems. SNNAP was designed as a tool for the rapid development and simulation of models of the activity of realistic single neurons or neural networks. Some advantages of the program are its ability to simulate common experimental manipulations such as injection of external currents into multiple cells, removal of

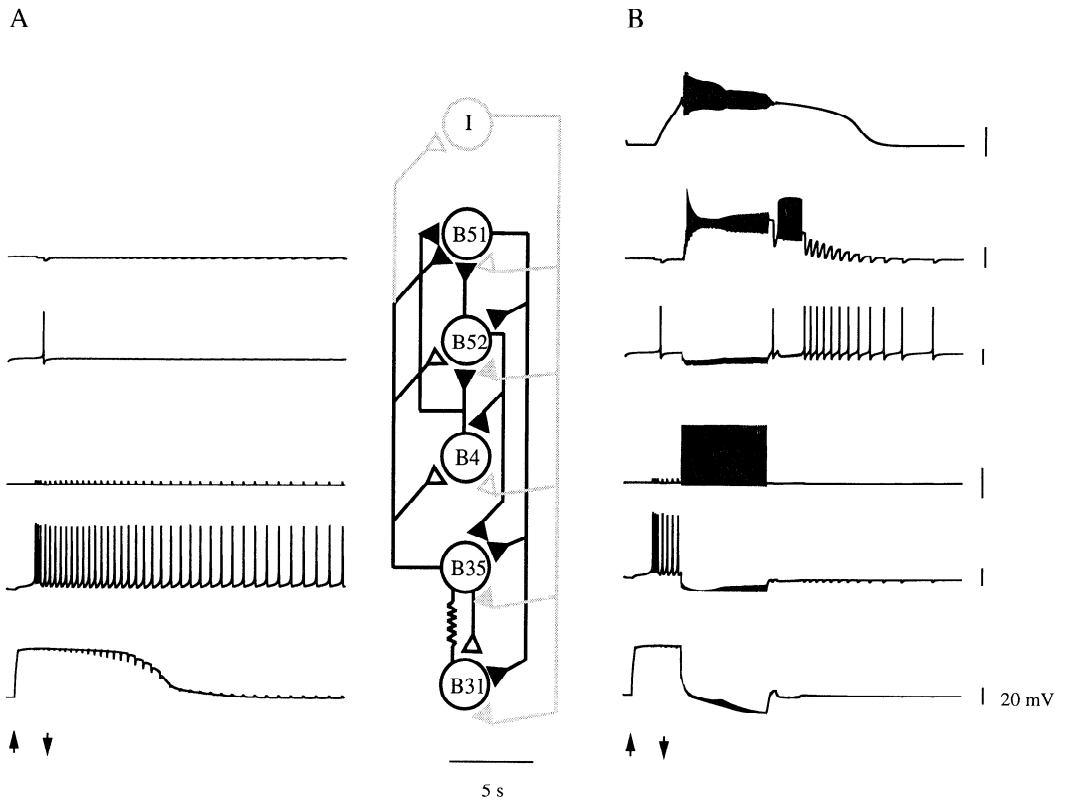

FIG. 8. Simulation of activity in a central pattern generator (CPG). Recent experimental work has identified several neurons in the buccal ganglia of *Aplysia* that are believed to function as a CPG. A network model of these neurons was developed to examine whether the known properties and synaptic connections of these neurons are sufficient to produce rhythmic neural activity. The biophysical properties of the simulated neurons and synaptic connections were derived from experimental data, and the parameters of the model are provided in Table 4. *A*: initial simulations incorporated the identified neurons *B4, B31, B35, B51,* and *B52.* Open triangles indicate excitatory synapses, and filled triangles indicate inhibitory synapses. A brief depolarizing current pulse (4.5 nA) was injected into nonspiking *cell B31* (onset and offset of the current are indicated by the arrows). Because of the intrinsic regenerative properties of *B31,* the depolarization of *B31* outlasts the duration of the current pulse. This depolarization of *B31* elicits a burst of spikes in electrically coupled *cell B35,* which because of its own intrinsic regenerative properties continues to fire after the depolarization of *B31* has decayed. The synaptic connections of *B35* elicit a single spike in *B52,* EPSPs in *B4,* and IPSPs in *B51.* The single spike in *B52* also elicits and IPSP in *B51* and *B4.* This network failed to simulate many features of neural activity that are observed experimentally in the buccal ganglia. For example, there is no burst of spikes in *cells B4* and *B51,* nor is the activity in *cells B31, B35,* and *B52* followed by a powerful inhibition. *B*: to simulate the observed patterns of neural activity in the buccal ganglia, it was necessary to incorporate an additional element into the CPG, *neuron I. Neuron I* was predicted to have intrinsic regenerative properties, make excitatory connections to *B4* and *B51,* inhibitory connections to *B31, B35,* and *B52,* and receive excitatory input from *B35.* In the modified network, the burst of spikes in *B35* produced summating EPSPs in *neuron I,* which eventually elicited a regenerative burst of activity in *cell I.* This activity in *cell I* produced the strong inhibition of *B31, B35,* and *B52* and elicited the burst of activity in *B4* and *B51.* The features of activity in the modified network are very similar to the pattern of activity in the buccal ganglia that has been termed Pattern 2 (Susswein and Byrne 1988; see also Baxter and Byrne 1991).

individual conductances to simulate pharmacological agents, modulation of membrane currents via application of modulatory transmitters, and voltage clamping cells. (Examples of voltage clamping were not shown.) In addition, an editor with a graphical interface can be used for easily specifying the structure of network, the intrinsic properties of the neurons, the type of the screen display and output files, and properties of the simulation, such as its duration and the timing of the various treatments. Little or no programming skills are necessary to use the simulator. The hierarchical organization of the input files (Fig. 2) allows for the creation of a library of modules describing different aspects of neural networks (such as descriptions of various voltage-dependent conductances, neurons, synaptic connections, or modulatory actions), thereby facilitating the generation of a new neuron or network from preexisting modules. The results of the simulation may then be viewed on-line or written to an output file.

The program can simulate different types of neurons with distinct biophysical properties and firing properties by including different voltage-dependent conductances (e.g., Figs. 3 and 5). Because the program allows for the calculation of the activation and inactivation functions with either the rate constant or the time constant method, it facilitates attempts to simulate neurons with parameters from the literature (Figs. 3*C* and 5). This successful replication of simulations from the literature also indicates that the methods used to simulate single neurons in SNNAP are valid.

The morphology of a neuron also is relevant to its electrical properties (e.g., Segev 1992), and SNNAP is capable of

TABLE 4. *Parameters for the buccal circuit*

Cell	C_M, μF	Conductance	E, mV	$\bar{g}$, μS	p	A/B	A_∞/B_∞ B_{min}	h	s	p	τ_A/τ_B, s τ_{max}	τ_{min}	h	s
						A. Intrinsic properties								
B31	0.006	Na	27.25	12.7	3	*A*		−14.9	3.17	1	2.5	0.7	−16.8	7.8
						B	0.0	−44.8	3.2	1	6.0	1.68	−16.75	7.0
		K	−77.8	0.4	2	*A*		−28.5	26.0	1	0.015	0.005	−41.55	2.9
						B	0.0	−57.1	23.3	1	0.14	0.05	−37.8	5.8
		K(M)	−97.8	7.2	1	*A*		14.25	0.9	1	0.028	0.0028	14.25	17.5
		Leak	−25.8	0.033										
B35	0.006	Na	45.7	5.0	3	*A*		−17.0	9.0	1	0.002	0.001	9.35	1.84
						B	0.0	−19.4	9.15	1	0.048	0.012	2.87	3.51
		K	−60.9	20.0	4	*A*		0.64	8.81	1	0.11	0.01	18.07	11.72
													−8.93	−11.2
						B	0.148	15.47	1.47	2	0.8	0.08	18.07	8.26
		Depolarized	9.97	0.8	3	*A*		−35.1	3.5	1	1.2	0.34	3.17	7.8
						B	0.0	−34.8	3.2	1	4.0	1.12	3.17	7.0
		Hyperpolarized-1	−70.9	20.2	3	*A*		−4.83	0.9	1	1.0	0.28	3.17	7.5
		Hyperpolarized-2	−95.9	15	3	*A*		−4.83	3.0	1	20.0	4.0	−5.17	1.0
		Leak	−43.0	0.18										
B52	0.002	Na	55.64	2.0	3	*A*		−33.1	4.8	1	0.0014	0.0004	−23.7	1.85
						B	0.0	−42.5	9.15	1	0.0119	0.0029	−30.2	3.51
		K	−62.0	13.0	4	*A*		−17.4	8.8	1	0.0027	0.0002	−15.0	11.72
													−42.0	−11.2
						B	0.148	−6.6	1.47	2	0.2	0.02	−15.0	8.26
		K(M)	−65.0	0.07	1	*A*		−32.4	9.3	1	13.6	3.26	−15.0	10.0
													−46.0	6.5
		Leak	−22.0	0.0095										
B51	0.0013	Na	53.7	2.3	4	*A*		−40.3	4.8	1	0.0014	0.0004	−30.64	1.85
						B	0.0	−49.4	9.15	1	0.0119	0.0029	−37.13	3.51
		K	−86.9	19.0	4	*A*		−29.4	8.81	1	0.0272	0.0022	−21.93	11.72
													−48.93	−11.2
						B	0.148	−14.5	1.47	2	0.2	0.02	−21.93	8.26
		Depolarized	−30.0	1.0	3	*A*		−57.1	12.5	1	2.3	0.64	−36.83	7.8
						B	0.0	−64.8	3.2	1	555.0	155.4	−36.83	7.0
		Hyperpolarized	−86.9	20.2	3	*A*		−34.8	0.9	1	50.0	14.0	−36.83	7.5
		Leak	−73.0	0.185										
B4	0.0013	Na	5.64	10.5	3	*A*		−18.1	6.0	1	0.0014	0.0004	−8.71	1.85
						B	0.0	−27.5	9.2	1	0.012	0.003	−15.2	3.51
		K	−95.0	12.0	4	*A*		−10.4	8.8	1	0.0272	0.0022	−0.0004	11.72
													−27.0	−11.2
						B	0.148	8.4	1.5	2	0.2	0.02	0.0014	8.26
		Leak	−39.8	0.24										
I	0.005	Na	75.71	2.3	3	*A*		−10.0	4.8	1	0.0056	0.0016	9.35	1.84
						B	0.0	−19.4	9.15	1	0.048	0.011	2.87	3.51
		K	−60.9	10.0	4	*A*		−5.0	8.81	1	0.055	0.0044	18.07	11.72
													−8.93	−11.2
						B	0.148	15.47	1.47	2	3.5	0.35	18.07	8.26
		Depolarized	9.97	0.8	3	*A*		−27.1	3.5	1	1.2	0.34	3.17	7.8
						B	0.0	−34.8	3.2	1	8.04	2.25	3.17	7.0
		Hyperpolarized	−56.9	20.2	3	*A*		−4.83	0.9	1	4.0	1.12	3.17	7.5
		Leak	−43.0	0.18										

Post	Pre	I_{syn} E, mV	$\bar{g}$, μS	A_{syn} τ, s	a	Post	Pre	I_{syn} E, mV	$\bar{g}$, μS	A_{syn} τ, s	a
					B. Connectivity						
B31	*B35*	40.0	0.1	0.01	9.15	*B52*	*B35*	−32.0	0.3	0.0006	0.5488
	B51	−60.0	0.04	0.009	8.232		*B4*	−70.0	0.05	0.0005	0.4574
	I	−70.7	1.0	0.04	36.59		*B51*	−55.0	0.2	0.0009	0.8232
B35	*B52*	−50.0	0.1	0.02	18.29		*I*	−80.0	0.3	0.001	0.915
	B51	−50.0	0.05	0.009	8.232	*B51*	*B35*	−72.0	0.2	0.07	64.03
	I	−60.0	1.0	0.02	18.29		*B4*	−75.0	0.5	0.02	18.29
B4	*B35*	−35.0	0.2	0.01	9.15		*B52*	−70.0	0.03	6.0	5488.3
	B52	−45.0	0.02	0.23	210.39			−75.0	1.0	0.06	54.88
	I	0.0	0.4	0.001	0.915		*I*	15.0	0.07	0.2	182.94
I	*B35*	30.0	0.015	1.0	914.72						

Neuron	Conductance	τ_{SM}, s	τ_{gbs}, s	b
		C. Modulation		
I	Depolarized	45.0	0.001	6.33

Explanations for *parts A, B,* and *C* are found in Tables 1, 2, and 3, respectively.

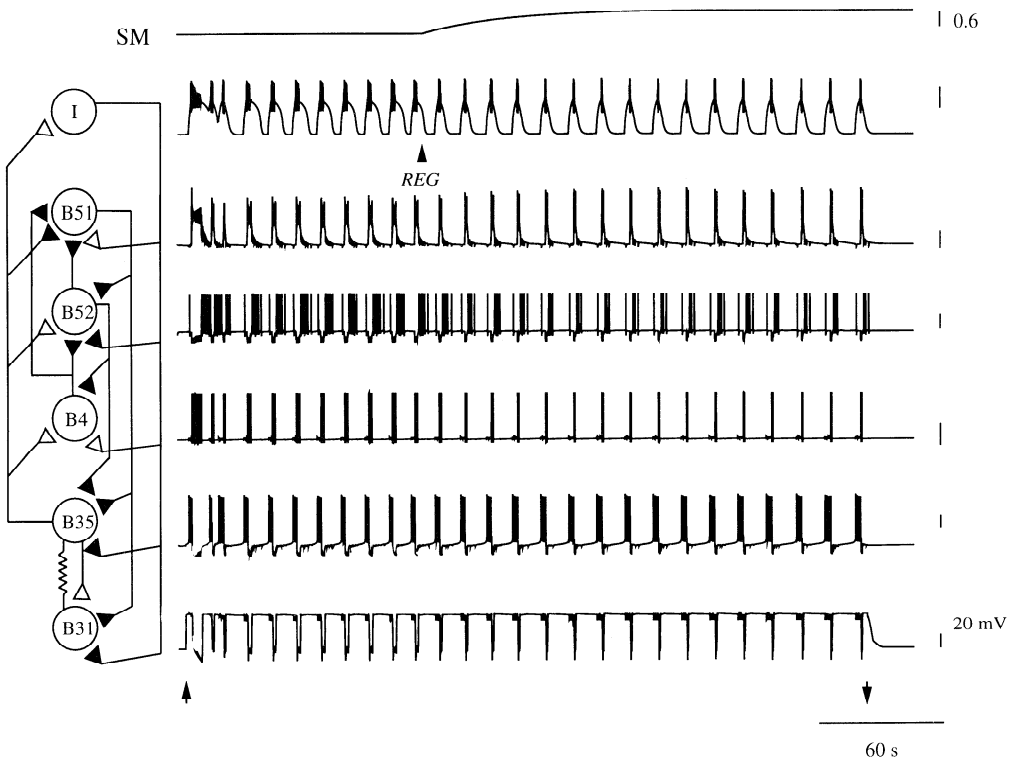

FIG. 9. Modulation of activity in the CPG. Sustained rhythmic activity in the CPG was induced by the injection of a constant depolarizing current (4.5 nA) into *cell B31* (onset and offset of the current are indicated by arrows). Patterned activity was initiated, which stabilized after 3 cycles. Ninety seconds later, the application (as indicated by an arrowhead) of an agent (REG) that modulates the slow inward conductance of *neuron I* was simulated. This led to an increase in the concentration of the 2nd messenger (SM) which gradually caused a reduction of the slow inward current of *neuron I*. As a result, more time was needed for *neuron I* to reach threshold for firing, and fewer spikes were fired during each burst. The general effect of the 2nd messenger was a lower frequency of the pattern and a reduction in the number of spikes per cycle.

simulating a branched neuron as a compartmental model. However, it is not capable of dealing with large-scale compartmental models, as is possible with other programs (e.g., GENESIS, NEURON, NeuronC, NODUS, SABER, and SPICE) and is currently limited to 30 compartments (e.g., Fig. 4*C*).

After creating different types of neurons, SNNAP (like some other programs, e.g., GENESIS and NODUS) can simulate small neural networks through different types of connections (Figs. 4, 6*B*, 7, and 8). A commonly used method for modeling chemical synaptic conductances is an equation (alpha function) that represents the explicit solution of a second-order ODE to an impulse (e.g., Rall 1967; Jack and Redman 1971; Wilson and Bower 1989). One disadvantage of the alpha function, it is the necessity to keep track of the timing of all the preceding spikes to correctly calculate postsynaptic conductances. This task becomes complicated as the number of synaptic conductances grows. Also, the use of this function precludes the incorporation of examples of synaptic modulation that are dependent on the duration of the presynaptic spike. To overcome these limitations, synaptic conductances in SNNAP are calculated by using the solution of the second-order ODE. This solution allows for the accurate summation of synaptic conductances (Fig. 4*A1*). In addition, changes in the spike duration are dynamically reflected in the amplitude of the PSPs (Fig. 6*B*). SNNAP also allows for the simulation of multicomponent synaptic actions (*Eq. 1*). This feature was used to simulate the slow as well as the fast components of the EPSPs in *Aplysia* motor neurons that mediate the tail-withdrawal reflex (White et al. 1991, 1993). In addition to chemical synapses, networks with electrically coupled cells can be simulated (Fig. 4*B*).

To accurately reconstruct the activity of a neural circuit, it is necessary to model not only the properties of individual neurons and synapses but also processes of modulation of voltage-dependent and synaptic conductances (Byrne 1987; Clarac et al. 1992; Hultborn and Kiehn 1992; Kandel 1985; Kupfermann 1991; Shepherd 1988). SNNAP incorporates equations that describe the modulation of voltage-dependent conductances by intrinsic pools of ions (e.g., Ca^{2+}) and second messengers (e.g., cAMP) that are regulated by external agents (e.g., 5-HT; Figs. 5, 6, and 8). These equations can also be used to simulate the effect of drugs (e.g., tetraethylammonium and tetrodotoxin) that block specific voltage-dependent conductances. It is difficult to compare SNNAP's ability to simulate modulatory effects with other simulators because there is little consideration of this issue in the literature. A recent review (De Schutter 1992) indicated that GENESIS, SABER, NEURON, and NODUS can simulate some forms of synaptic plasticity, however. SNNAP simulates aspects of synaptic plasticity in two ways. First, changes in transmitter release can be regulated by modulating the duration of the action potential. Thus a modulatory agent, by regulating a voltage-dependent conductance that affects spike duration, can

affect release (e.g., Fig. 6*B*). SNNAP can also be used to simulate spike frequency–dependent release and changes in release that are dependent on the steady state of the membrane potential. Second, transmitter release can be regulated by direct modulation. Currently our implementation only includes a description of synaptic depression that is based on a simple depletion-type model (*Eq. 9* and Fig. 7). Future modifications of SNNAP will incorporate more accurate descriptions of the release process, including descriptions of multiple pools of transmitters as well as direct second-messenger and ion-dependent regulation of the release process (e.g., Gingrich and Byrne 1985, 1987).

SNNAP[1] may be useful to both experimentalists and theoreticians who wish to integrate electrophysiological information into a real-time dynamic simulation of physiological patterns of activity in neurons and networks. Currently, we are using SNNAP to model the CPG in the buccal ganglia of *Aplysia* (Figs. 8 and 9) (Ziv et al. 1991, 1992) and the circuit that controls the tail-withdrawal reflex in *Aplysia* (White et al. 1991, 1993). This simulator may also be a useful tool for teaching several aspects of neuroscience such as the ionic basis of action potentials and neuronal excitability, current flow in dendritic trees, synaptic transmission, and the properties of simple neural networks and their modulation by extrinsic factors (Baxter et al. 1993).

We thank J. X. Kong for programming assistance and Dr. J. Raymond for helpful comments on the manuscript.

This research was supported by Air Force Office of Scientific Research Grant 91-0027 and Award KO5-MH00649.

Address for reprint requests: J. H. Byrne, Dept. of Neurobiology and Anatomy, University of Texas Medical School at Houston, 6431 Fannin, Houston, TX 77225.

Received 18 May 1993; accepted in final form 16 August 1993.

REFERENCES

BAXTER, D. A. AND BYRNE, J. H. Serotonergic modulation of two potassium currents in the pleural sensory neurons of *Aplysia*. *J. Neurophysiol.* 62: 665–679, 1989.

BAXTER, D. A. AND BYRNE, J. H. Mathematical modeling of the serotonergic modulation of electrophysiological properties of sensory neurons in *Aplysia*. *Soc. Neurosci. Abstr.* 16: 1297, 1990.

BAXTER, D. A. AND BYRNE, J. H. Synaptic interactions among pattern generating neurons in buccal ganglia of *Aplysia*. *Soc. Neurosci. Abstr.* 17: 124, 1991.

BAXTER, D. A., ZIV, I., AND BYRNE, J. H. Simulator for neural networks and action potentials (SNNAP): use of computer simulations as a supplement for undergraduate and graduate courses in neurobiology. *Soc. Neurosci. Abstr.* 19: 208, 1993.

BONEY, D. G., FEINSWOG, L. J., HUTSON, K., KENYON, G. T., AND TAM, D. C. An object-oriented paradigm for simulating interconnected neural systems. *Soc. Neurosci. Abstr.* 17: 126, 1991.

BUNOW, B., SEGEV, I., AND FLESHMAN, J. W. Modeling the electrical behavior of anatomically complex neurons using a network analysis program: excitable membrane. *Biol. Cybern.* 53: 41–56, 1985.

BYRNE, J. H. Analysis of ionic conductance mechanisms in motor cells mediating inking in *Aplysia californica*. *J. Neurophysiol.* 43: 630–650, 1980a.

BYRNE, J. H. Quantitative aspects of ionic conductance mechanisms contributing to firing pattern of motor cells mediating inking behavior in *Aplysia californica*. *J. Neurophysiol.* 43: 651–668, 1980b.

BYRNE, J. H. Neural circuit for inking behavior in *Aplysia californica*. *J. Neurophysiol.* 43: 896–911, 1980c.

BYRNE, J. H. Cellular analysis of associative learning. *Physiol. Rev.* 67: 329–439, 1987.

BYRNE, J. H., CLEARY, L. J., AND BAXTER, D. A. Aspects of the neural and molecular mechanisms of short term sensitization of *Aplysia*: modulatory effects of serotonin and cAMP on duration of action potentials, excitability and membrane currents in tail sensory neurons. In: *The Biology of Memory*, edited by L. R. Squire and E. Lindenlaub. Stuttgart, Germany: Schattauer, 1990, p. 7–28.

BYRNE, J. H., ZWARTJES, R., HOMAYOUNI, R., CRITZ, S. D., AND ESKIN, A. Roles of second messenger pathways in neuronal plasticity and in learning and memory: insights gained from *Aplysia*. *Adv. Second Messenger Phosphoprotein Res.* 27: 47–108, 1993.

CANAVIER, C. C., BAXTER, D. A., CLARK, J. W., AND BYRNE, J. H. Simulations of action potentials, transmitter release, and plasticity of sensorimotor synapses in *Aplysia*. *Soc. Neurosci. Abstr.* 17: 1590, 1991.

CAREW, T. J. AND SAHLEY, C. J. Invertebrate learning and memory: from behavior to molecules. *Annu. Rev. Neurosci.* 9: 435–487, 1986.

CARNEVALE, N. T., WOOLF, T. B., AND SHEPHERD, G. M. Neuron simulation with SABER. *J. Neurosci. Methods* 33: 135–148, 1990.

CLARAC, F., EL MANIRA, A., AND CATTAERT, D. Presynaptic control as a mechanism of sensory-motor integration. *Curr. Opin. Neurobiol.* 2: 764–769, 1992.

COUGHANOWR, D. R. AND KOPPEL, L. B. Higher-order systems: second-order and transportation lag. In: *Process Systems Analysis and Control*, edited by D. R. Coughanowr and L. B. Koppel. New York: McGraw-Hill, 1975, p. 83–98.

DE SCHUTTER, E. Computer software for development and simulation of compartmental models of neurons. *Comput. Biol. Med.* 19: 71–81, 1989.

DE SCHUTTER, E. A consumer guide to neuronal modeling software. *Trends Neurosci.* 15: 462–464, 1992.

EPSTEIN, I. R. AND MARDER, E. Multiple modes of a conditional neural oscillator. *Biol. Cybern.* 63: 25–34, 1990.

GETTING, P. A. Reconstruction of small neural networks. In: *Methods in Neuronal Modeling*, edited by C. Koch and I. Segev. Cambridge, MA: MIT Press, 1989, p. 171–194.

GINGRICH, K. J. AND BYRNE, J. H. Simulation of synaptic depression, posttetanic potentiation and presynaptic facilitation of synaptic potentials from sensory neurons mediating gill-withdrawal reflex in *Aplysia*. *J. Neurophysiol.* 53: 652–669, 1985.

GINGRICH, K. J. AND BYRNE, J. H. Single-cell neuronal model for associative learning. *J. Neurophysiol.* 57: 1705–1715, 1987.

HINES, M. A program for simulation of nerve equations with branching geometries. *Int. Biomed. Comput.* 24: 55–68, 1989.

HOCHNER, B., KLEIN, M., SCHACHER, S., AND KANDEL, E. R. Action potential duration and the modulation of transmitter release from the sensory neuron of *Aplysia* in presynaptic facilitation and behavioral sensitization. *Proc. Natl. Acad. Sci. USA* 83: 8410–8414, 1986.

HODGKIN, A. L. AND HUXLEY, A. F. A Quantitative description of membrane current and its application to conduction and excitation in nerve. *J. Physiol. Lond.* 117: 500–544, 1952.

HULTBORN, H. AND KIEHN, O. Neuromodulation of vertebrate motor neuron membrane properties. *Curr. Opin. Neurobiol.* 2: 770–775, 1992.

HURWITZ, I., GOLDSTEIN, R. S., AND SUSSWEIN, A. J. A network of cells initiating patterned activity in the buccal ganglia of *Aplysia*. *Soc. Neurosci. Abstr.* 19: 1700, 1993.

JACK, J. J. B. AND REDMAN, S. J. The propagation of transient potentials in some linear cable structures. *J. Physiol. Lond.* 215: 283–320, 1971.

KANDEL, E. R. Cellular mechanisms of learning and the biological basis of individuality. In: *Principles of Neural Science*, edited by E. R. Kandel and J. H. Schwartz. New York: Elsevier, 1985, p. 816–833.

KANDEL, E. R. AND SCHWARTZ, J. H. Molecular biology of learning: modulation of transmitter release. *Science Wash. DC* 218: 433–443, 1982.

KLEIN, M., COMARDO, J., AND KANDEL, E. R. Serotonin modulates a specific potassium current in the sensory neurons that show presynaptic facilitation in *Aplysia*. *Proc. Natl. Acad. Sci. USA* 79: 5713–5717, 1982.

KLEIN, M. AND KANDEL, E. R. Presynaptic modulation of voltage-dependent Ca^{2+} current: mechanism for behavioral sensitization in *Aplysia*. *Proc. Natl. Acad. Sci. USA* 75: 3512–3516, 1978.

KUPFERMANN, I. Learning and memory. In: *Principles of Neural Science*, edited by E. R. Kandel, J. H. Schwartz, and T. M. Jessell. New York: Elsevier, 1991, p. 997–1008.

MILTON, J. G., VAN DER HEIDEN, U., LONGTIN, A., AND MACKEY, M. C. Complex dynamics and noise in simple neural networks with delayed mixed feedback. *Biomed. Biochim. Acta* 49: 697–707, 1990.

[1] To obtain copies of the program, interested individuals may write to the authors. e-mail: jbyrne@nba19.med.uth.tmc.edu

PLUMMER, E. R. AND KIRK, M. D. Premotor neurons B51 and B52 in the buccal ganglia of *Aplysia californica:* synaptic connections, effects on ongoing motor rhythms and peptide modulation. *J. Neurophysiol.* 63: 539–558, 1990.

PRESS, W. H., TEUKOLSKY, S. A., VETTERLING, W. T., AND FLANNERY, B. P. Integration of ordinary differential equations. In: *Numerical Recipes in C,* edited by W. H. Press, S. A. Teukolsky, W. T. Vetterling, and B. P. Flannery. Cambridge, UK: Cambridge Univ. Press, 1992, p. 707–752.

RALL, W. Distinguishing theoretical synaptic potentials computed for different soma-dendritic distributions of synaptic inputs. *J. Neurophysiol.* 30: 1138–1168, 1967.

RALL, W. Cable theory for dendritic neurons. In: *Methods in Neuronal Modeling,* edited by C. Koch and I. Segev. Cambridge, MA: MIT Press, 1989, p. 9–62.

SEGEV, I. Single neuron models: oversimple, complex and reduced. *Trends Neurosci.* 15: 414–421, 1992.

SEGEV, I., FLESHMAN, J. W., AND BURKE, R. E. Compartmental models of complex neurons. In: *Methods in Neuronal Modeling,* edited by C. Koch and I. Segev. Cambridge, MA: MIT Press, 1989, p. 63–96.

SHEPHERD, G. M. Learning and memory. In: *Neurobiology,* edited by G. M. Shepherd. New York: Oxford Univ. Press, 1988, p. 584–610.

SMITH, R. G. Neuron C: a computational language for investigating functional architecture of neural circuits. *J. Neurosci. Methods* 43: 83–108, 1992.

SUGITA, S., GOLDSMITH, J. R., BAXTER, D. A., AND BYRNE, J. H. Involvement of protein kinase C in serotonin-induced spike broadening and synaptic facilitation in sensorimotor connections of *Aplysia. J. Neurophysiol.* 68: 643–651, 1992.

SUSSWEIN, A. J. AND BYRNE, J. H. Identification and characterization of neurons initiating patterned neural activity in the buccal ganglia of *Aplysia. J. Neurosci.* 8: 2049–2061, 1988.

WANG, D. AND HSU, C. SLONN: A simulation language for modeling of neural networks. *Simulation.* 55: 69–83, 1990.

WHITE, J. A., CLEARY, L. J., ZIV, I., AND BYRNE, J. H. A network model of the tail-withdrawal circuit in *Aplysia. Soc. Neurosci. Abstr.* 17: 1590, 1991.

WHITE, J. A., ZIV, I., CLEARY, L. J., BAXTER, D. A., AND BYRNE, J. H. The role of interneurons in controlling the tail-withdrawal reflex in *Aplysia:* a network model. *J. Neurophysiol.* 70: 1777–1786, 1993.

WILSON, M. A. AND BOWER, J. M. The simulation of large-scale neural networks. In: *Methods in Neuronal Modeling,* edited by C. Koch and I. Segev. Cambridge, MA: MIT Press, 1989, p. 291–334.

ZIV, I., BAXTER, D. A., AND BYRNE, J. H. Simulator for neural networks and action potentials (SNNAP): application to a central pattern generator. *Soc. Neurosci. Abstr.* 17: 125, 1991.

ZIV, I., BAXTER, D. A., AND BYRNE, J. H. Network model of a central pattern generator in the buccal ganglia of *Aplysia. Soc. Neurosci. Abstr.* 18: 1279, 1992.